Isomerization Behavior in the (π-Allyl)palladium(II) Complexes with N^{21},N^{22}-Bridged Porphyrin Ligands

Yuko Takao,*,† Tokuji Takeda,† Jun-ya Watanabe,‡ and Jun-ichiro Setsune*,‡

Osaka Municipal Technical Research Institute, Joto-ku, Osaka 536-8553, Japan, and Department of Chemistry, Faculty of Science, and Graduate School of Science and Technology, Kobe University, Nada-ku, Kobe 657-8501, Japan

Received July 12, 2002

Reactions of (dichloro)palladium(II) complexes of N^{21},N^{22}-etheno-bridged porphyrins with $AgClO_4$ gave bis(perchlorato)Pd^{II} porphyrins. These complexes reacted with allyltributyltins to afford a mixture of cis and trans isomers of (π-allyl)Pd^{II}(porphyrin). The trans isomer of (π-C_3H_5)Pd^{II}(porphyrin) preferentially formed by the reaction of (η^1-C_3H_5)$SnBu_3$ gradually isomerized to a cis isomer with exchange between two syn positions and between two anti positions, reaching an equilibrium state with an trans/cis ratio of 3:7. The $\Delta G^{\ddagger}_{298}$ value (91.2 kJ/mol) for this syn-syn−anti-anti exchange is much greater than that reported for ordinary nitrogen base ligands such as phenanthroline. This is ascribed to the steric hindrance of the porphyrin ligand. The syn/anti exchange via an (η^1-allyl)Pd intermediate was also observed in the interconversion of (η^3-butenyl)Pd^{II}(porphyrin). The ratio between isomers with the *trans*-2-butenyl ligand and the *cis*-2-butenyl ligand from the preparation at room temperature in CH_2Cl_2 was 68:32, and the $\eta^3-\eta^1$ type isomerization on warming at 80 °C in d_6-DMSO established an equilibrium state with a ratio of 96:4. The single-crystal X-ray analysis of the cis isomer of (η^3-C_3H_5)Pd^{II}(porphyrin) showed an average Pd−C bond distance of 2.119(3) Å. The N3−Pd−N4 plane is canted by 53.4° from the porphyrin plane defined by the four meso carbons C5, C10, C15, and C20. The π-allyl plane has a dihedral angle of 106.8° relative to the N3−Pd−N4 plane and of 53.5° relative to the porphyrin plane.

Introduction

Remarkable progress has been made in the chemistry of organopalladium complexes with various amine and phosphine ligands; those with bidentate nitrogen base ligands have recently been recognized as useful in enantioselective organic transformations and polymerizations.[1,2] A coordination site for an organo ligand, however, is not available for ordinary palladium porphyrins because of the tetradentate nature of porphyrin. Therefore, porphyrin has never been well-known to organopalladium chemists, despite its potential in stereochemical effects and NMR ring current effects. The utility of the latter effects has been recognized for five-coordinated and six-coordinated organometallic porphyrin complexes.[3] Proton NMR signals due to the metal-bound organic ligand undergo low-frequency shifts depending on the distance and direction from the center of the porphyrin ring. For example, ring current effects for the metal-bound methyl protons amount to more than 5 ppm.[3b,c] Callot and co-workers reported Pd complexes of N^{21},N^{22}-methano-bridged porphyrin.[4] However, they have never been used for organopalladium chemistry due to their labile nature. We have recently shown that N^{21},N^{22}-etheno-bridged porphyrin serves as a bidentate nitrogen base ligand for stable coordination to palladium.[5] The present report is concerned with the synthesis and isomerization behavior of (π-allyl)palladium derivatives with N^{21},N^{22}-bridged porphyrin ligands, and the roles of porphyrin ligands in controlling cis−trans isomerization and also in the spectroscopic characterization of (π-allyl)palladium complexes will be discussed in detail.[6]

† Osaka Municipal Technical Research Institute.
‡ Kobe University.

(1) (a) Müller, D.; Umbricht, G.; Weber, B.; Pfaltz, A. *Helv. Chim. Acta* **1991**, *74*, 232. (b) Togni, A. *Tetrahedron: Asymmetry* **1991**, *2*, 683. (c) Pfaltz, A. *Acc. Chem. Res.* **1993**, *26*, 339. (d) Kubota, H.; Nakajima, M.; Koga, K. *Tetrahedron Lett.* **1993**, *34*, 8135. (e) Togni, A.; Venanzi, L. M. *Angew. Chem., Int. Ed. Engl.* **1994**, *33*, 497. (f) Tanner, D.; Andersson, P. G.; Harden, A.; Somfai, P. *Tetrahedron Lett.* **1994**, *35*, 4631. (g) Gamez, P.; Dunjic, B.; Fache, F.; Lemaire, M. *J. Chem. Soc., Chem. Commun.* **1994**, 1417. (h) Bolm, C.; Kaufmann, D.; Zehnder, M.; Neuburger, M. *Tetrahedron Lett.* **1996**, *37*, 3985. (i) Oslob, J. D.; Åkermark, B.; Helquist, P.; Norrby, P. O. *Organometallics* **1997**, *16*, 3015.

(2) (a) Johnson, L. K.; Mecking, S.; Brookhart, M. *J. Am. Chem. Soc.* **1996**, *118*, 267. (b) Rix, F. C.; Brookhart, M.; White, P. S. *J. Am. Chem. Soc.* **1996**, *118*, 2436. (c) Rix, F. C.; Brookhart, M.; White, P. S. *J. Am. Chem. Soc.* **1996**, *118*, 4746. (d) Brookhart, M.; Wagner, M. I. *J. Am. Chem. Soc.* **1996**, *118*, 7219. (e) LaPointe, A. M.; Rix, F. C.; Brookhart, M. *J. Am. Chem. Soc.* **1997**, *119*, 906. (f) Delis, J. G. P.; Aubel, P. G.; Vrieze, K.; van Leeuwen, P. W. N. M.; Veldman, N.; Spek, A. L.; van Neer, F. J. R. *Organometallics* **1997**, *16*, 2948. (g) Mecking, S.; Johnson, L. K.; Wang, L.; Brookhart, M. *J. Am. Chem. Soc.* **1998**, *120*, 888.

(3) (a) Guilard, R.; Tabard, A.; van Caemelbecke, E.; Kadish, K. M. In *The Porphyrin Handbook*; Kadish, K. M., Smith, K. M., Guilard, R., Eds.; Academic Press: New York, 2000; Vol. 3, p 295. (b) Clarke, D. A.; Dolphin, D.; Grigg, R.; Johnson, A. W.; Pinnock, H. A. *J. Chem. Soc. C* **1968**, 881. (c) Ogoshi, H.; Setsune, J.; Omura, T.; Yoshida, Z.-I. *J. Am. Chem. Soc.* **1975**, *97*, 6461.

(4) Callot, H. J.; Fischer, J.; Weiss, R. *J. Am. Chem. Soc.*, **1982**, *104*, 1272.

(5) (a) Takao, Y.; Takeda, T.; Miyashita, K.; Setsune, J. *Chem. Lett.* **1996**, 761. (b) Takao, Y.; Takeda, T.; Setsune, J. *Bull. Chem. Soc. Jpn.* **1998**, *71*, 1327.

(6) Preliminary communication of this paper: Takao, Y.; Takeda, T.; Jun-ya, W.; Setsune, J. *Organometallics* **1999**, *18*, 2936.

10.1021/om0205593 CCC: $25.00
Publication on Web 12/14/2002

Table 1. ^{1}H NMR Chemical Shifts (δ) for π-Allyl Moieties of (π-Allyl)palladium(II) Porphyrins 3a−5a in $CDCl_3$

compd	central CH	terminal CH	other protons
cis-**3a**	2.14 (m, 1H)	−0.28 (d, 2H, J_{syn} = 6.9 Hz) −4.55 (d, 2H, J_{anti} = 11.9 Hz)	
trans-**3a**	−1.25 (m, 1H)	−1.37 (d, 2H, J_{syn} = 5.9 Hz) −1.06 (d, 2H, J_{anti} = 10.9 Hz)	
cis-**4a**	2.64 (s, 1H)	1.10 (s, 2H)	−1.69, −5.38 (d × 2, 2H × 2, J_{gem} = 12.9 Hz, CH_2)
trans-**4a**	−1.68 (s, 1H)	0.27 (s,2H)	−0.91, −1.19 (d × 2, 2H × 2, J_{gem} = 13.9 Hz, CH_2)
cis(*cis*)-**5a**	3.47[b] (m, 1H)	−0.91 (d, 1H, J_{syn} = 6.6 Hz) −3.05 (d, 1H, J_{anti} = 12.7 Hz) 0.96[b] (m, 1H)	−3.77 (d, 3H, CH_3)
cis(*trans*)-**5a**	2.03 (m, 1H)	−0.50 (d, 1H, J_{syn} = 6.6 Hz) −4.77 (d, 1H, J_{anti} = 12.0 Hz) −3.62 (m, 1H)	−1.10 (d, 3H, CH_3)
trans(*cis*)-**5a**	−1.43 (m, 1H)	−1.43[a] −0.77[a] −0.77[a]	−1.54 (d, 3H, CH_3)
trans(*cis*)-**5a**[c]	−1.43 (dt, 1H, J_{syn} = 6.9 Hz, J_{anti} = 12.6 Hz)	−1.54 (d, 1H, J_{syn} = 6.9 Hz) −0.64 (d, 1H, J_{anti} = 12.6 Hz) −0.85 (dq, 1H, J_{syn} = 6.9 Hz)	
trans(*trans*)-**5a**		−1.90 (d, 1H, J_{syn} = 5.1 Hz) −1.28 (d, 1H, J_{anti} = 12.1 Hz) 0.21[b] (m, 1H)	−1.60 (d, 3H, CH_3)

[a] Signals are overlapped. [b] Not proved. [c] In d_6-DMSO.

Results and Discussion

Synthesis of (π-Allyl)palladium(II) Porphyrins. Nucleophilic displacement of the coordinated halide ion by allyl anion is one of the most important methods for synthesizing (π-allyl)palladium(II) complexes. Allylsilanes and allyltins, convenient reagents as masked allyl anions, were treated with dichloropalladium(II) complexes of (1,2-disubstituted etheno-N^{21},N^{22})porphyrins, such as (N^{21},N^{22}-PhC═CPh-TPP)$PdCl_2$ (**1a**),[7] (N^{21},N^{22}-PhC═CPh-OEP)$PdCl_2$ (**1b**),[7] and (N^{21},N^{22}-EtC═CEt-TPP)$PdCl_2$ (**1c**). Since these Pd(II) porphyrins did not react with these reagents in $CHCl_3$ at room temperature, the reactivity of Pd was increased by the addition of over 2-fold molar amounts of $AgClO_4$ to **1a**−**c**. The displacement of the coordinated chlorides gave the bis(perchlorate) compounds **2a**−**c** quantitatively, as is generally seen in Pd chemistry. A broad 4H signal at 0.35 ppm in the ^{1}H NMR spectrum of **2a** disappeared by adding D_2O. Therefore, this signal is associated with two water molecules coordinated to Pd(II). (π-C_3H_5)Pd^{II} complexes **3a**,**b** were synthesized in 93% and 55% isolated yields, respectively, by the reaction of **2a**,**b** with (η^1-C_3H_5)$SnBu_3$ (1.1 equiv) for 3 h in CH_2Cl_2. The (π-C_3H_5)Pd^{II} complex as a chloride (**3a′**) was obtained alternatively by the reaction of N^{21},N^{22}-PhC═CPh-TPP) free base with $[Pd(C_3H_5)Cl]_2$ (1.1 equiv) in benzene at room temperature overnight in a 90% isolated yield. These (π-allyl)Pd^{II} porphyrins are composed of two conformational isomers with respect to the apparent π-allyl ligand rotation. The ^{1}H NMR signals of the π-allyl group in **3a**,**b** are observed as two C_s-symmetric sets with a ratio of 3:7 at low-frequency regions. Their chemical shifts are influenced greatly by the ring current effect of porphyrin (Table 1). The major component of **3a** shows the signals due to the allyl terminal methylene protons H_{anti} at −4.55 (J_{anti} = 11.9 Hz) and H_{syn} at −0.28 ppm (J_{syn} = 6.9 Hz) and the signal due to the allyl central methine proton H_{cent} at 2.14 ppm. Thus, it was identified as a cis isomer (*cis*-**3a** in Scheme 1) because the terminal methylene protons H_{anti} are estimated to be very close to the porphyrin plane on the basis of the low-frequency chemical shift. The minor component shows H_{anti} at −1.06 ppm (J_{anti} = 10.9

Scheme 1

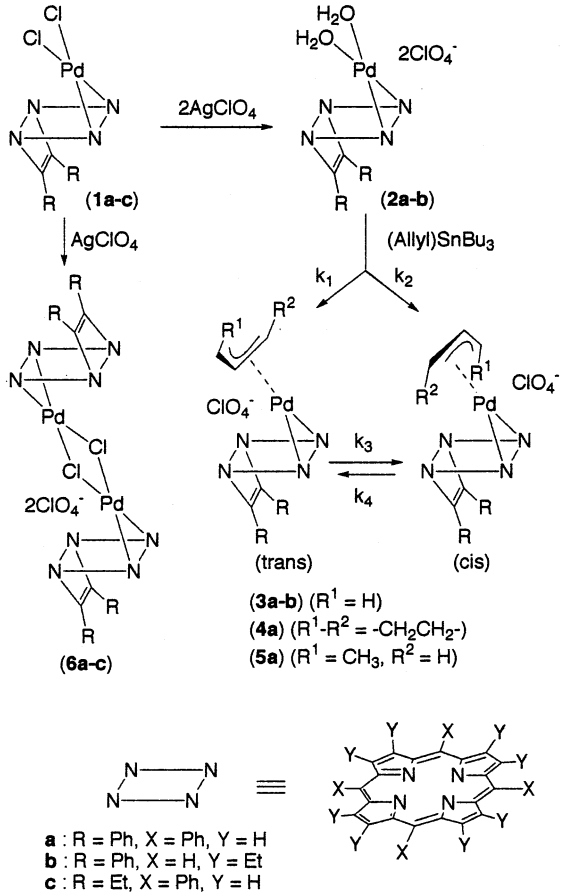

(7) Abbreviations: TPP = 5,10,15,20-tetraphenylporphyrin dianion; OEP = 2,3,7,8,12,13,17,18-octaethylporphyrin dianion.

Hz), H_{syn} at −1.37 ppm (J_{syn} = 5.9 Hz), and H_{cent} at −1.25 ppm. The H_{cent} resonates at a 3.39 ppm lower chemical shift and the H_{anti} appears at a 3.49 ppm higher chemical shift than the corresponding protons of *cis*-**3a**. This minor component was identified as a trans isomer, because H_{cent} comes closer to the porphyrin plane, rather than H_{anti} and H_{syn}.

Reaction of **2a** with (cyclopent-2-enyl)tributyltin afforded the corresponding (π-allyl)Pd^{II} derivative **4a** in 93% yield as a mixture of cis and trans conformational isomers. The ^{1}H NMR chemical shifts of the allyl central methine proton at 2.64 and −1.68 ppm are very similar to those of *cis*-**3a** and *trans*-**3a**, and therefore, these signals are associated with cis and trans isomers, respectively. The $-CH_2CH_2-$ part of the π-cyclopentenyl ligand of *cis*-**4a** is very close to the porphyrin plane, as judged from the remarkably low frequency signals at −5.38 and −1.69 ppm. The (π-butenyl)Pd^{II} complex **5a** was similarly obtained in 90% yield when **2a** was allowed to react with (2-butenyl)tributyltin overnight. Since we have used a mixture of *cis*- and *trans*-2-butenyltin reagents, there should arise four stereochemical isomers in this case. In the ^{1}H NMR spectrum obtained after chromatographic purification, four sets of signals due to the π-butenyl group are observed, including four methyl signals at −1.10, −1.54, −1.60, and −3.77 ppm with a ratio of 61:29:7:3. Each set of the π-butenyl signals can be associated with one of the four possible isomers of **5a** on the basis of the coupling constants and chemical shifts. The component with the methyl signal at −1.10 ppm shows the allyl central methine proton at 2.03 ppm, which is very similar to the corresponding chemical shift of *cis*-**3a**. Furthermore, there are two anti protons of the allyl terminal positions, and their chemical shifts at −4.77 and −3.62 ppm are in the range characteristic of the cis conformation. These NMR features are consistent with the cis isomer of a *trans*-π-butenyl configuration (*cis*(*trans*)-**5a**). In one of the other three components, the extremely high ^{1}H NMR chemical shifts at −3.77 and −3.05 ppm of the methyl group and of the anti protons, respectively, at the allyl terminal positions are indicative of the *cis*-π-butenyl configuration in the cis conformation, which is designated as *cis*(*cis*)-**5a**. The other two components with the methyl signal at −1.54 and −1.60 ppm show signals due to the π-allyl protons in a frequency region similar to that of *trans*-**3a**. The component with the methyl signal at −1.54 ppm shows the allyl central methine proton as a doublet (J_{anti} = 12.6 Hz) of triplets (J_{syn} = 6.9 Hz) in d_6-DMSO. This is indicative of the *cis*-π-butenyl configuration in the trans conformation (*trans*(*cis*)-**5a**). The remaining component with the methyl signal at −1.60 ppm is therefore associated with the *trans*(*trans*)-**5a** isomer.

When **1a**−**c** was reacted with an equimolar amount of $AgClO_4$, one chloride was displaced to afford the mono(perchlorate) species **6a**−**c** in quantitative yield. Since the ^{1}H NMR spectra of **6a**−**c** show a C_s-symmetric signal pattern as well as those for bis(perchlorate) species **2a**−**c**, these mono(perchlorate) compounds are considered to have a (μ-dichloro)dipalladium(II) bis(porphyrin) structure. The ^{1}H chemical shifts of the porphyrin periphery of **6a**−**c** are remarkably lower than those of the monomeric derivatives due to the shielding

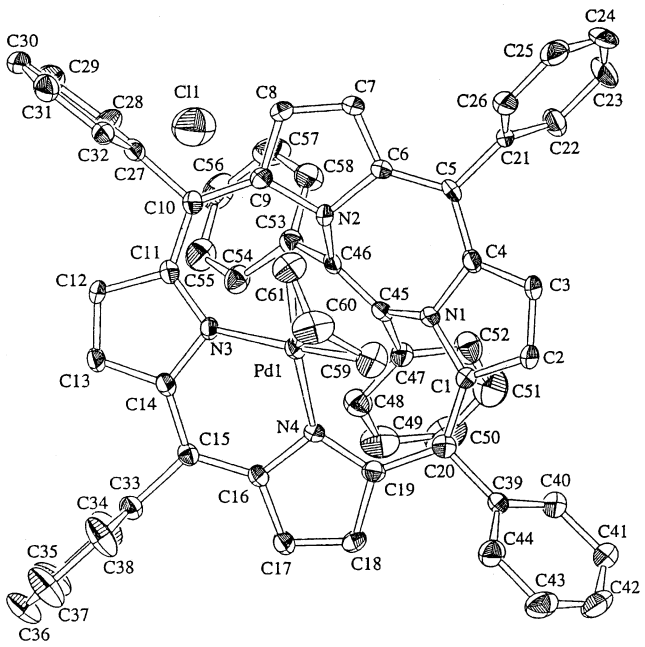

Figure 1. ORTEP drawing of *cis*-**3a′** with 50% thermal ellipsoids.

effect of porphyrin. Comparisons of the pyrrole-β protons of **6a** (9.41, 8.49, 8.47, 7.69 ppm) and **2a** (9.35, 8.91, 8.68, 8.20 ppm), of the meso protons of **6b** (10.77, 10.20, 9.15 ppm) and **2b** (11.14, 10.59, 10.12 ppm), and of the methyl protons of **6b** (1.38, 1.15, 0.97, 0.94 ppm) and **2b** (2.31, 1.85, 1.39, 1.25 ppm) nicely illustrate the presence of an additional ring current effect derived from the dimeric structure. Further support for the dimeric structure was obtained by MS spectra of **6b** and **6c**. The ESI-MS spectrum of **6a** in methanol showed a principal peak at *m*/*z* 963.1429 that corresponds to a mononuclear complex with a methanol ligand, [(N^{21},N^{22}-PhC═CPh-TPP)PdCl(MeOH)]$^+$ (*m*/*z* 963.2093). On the other hand, the dinuclear structure of **6b** was retained under the same ESI-MS conditions in methanol. The observed main peak at *m*/*z* 852.2066 is in good agreement with the theoretical peak for {[(N^{21},N^{22}-PhC═CPh-OEP)PdCl]$_2$}$^{2+}$ (*m*/*z* 852.3082). Although **6a** did not show signals due to the dicationic bis(porphyrin) in the FABMS measurement, a monocationic dinuclear species, {[(N^{21},N^{22}-PhC═CPh-TPP)PdCl]$_2$(ClO_4)}$^+$ (*m*/*z* 1773), was observed.

A vacant coordination site of Pd is not available in the case of the mono(perchlorate), and **6a** did not react with allyltributyltin in CH_2Cl_2 at room temperature.

Structures. Recrystallization of a trans/cis (3:7) mixture of [(1,2-diphenyletheno-N^{21},N^{22})-*meso*-tetraphenylporphyrinato-*N*,$^{23}N^{24}$](η^3-allyl)palladium(II) chloride (**3a′**) from CH_2Cl_2−Et_2O gave crystals of *cis*-**3a′** only. This is probably due to the effect of crystal packing. The X-ray molecular structure of *cis*-**3a′** and the crystallographic data are shown in Figure 1 and Table 2, respectively. Table 3 exhibits selected distances, angles, and dihedral angles between least-squares planes for *cis*-**3a′**. The Pd−N (2.106−2.118 Å) and Pd−C (2.085−2.147 Å) bond lengths as well as the N3−Pd−N4 (83.4°) and C59−Pd−C61 (68.7°) bite angles are similar to those of the (π-allyl)palladium complex of 2,2′-bipyridine.[8−10] The four coordinating atoms (N3, N4, C59, C61) of Pd constitute a square-planar coordination

Table 2. Crystallographic Data for *cis*-3a′

formula	$C_{61}H_{43}N_4ClPd\cdot 2H_2O$
fw	1009.92
cryst size/mm	0.4 × 0.4 × 0.1
T/K	299
cryst syst	monoclinic
space group	$P2_1/n$
a/Å	16.518(1)
b/Å	16.287(3)
c/Å	18.134(2)
β/deg	92.706(7)
V/Å^3	4873(1)
Z	4
D_{calcd}/g cm^{-3}	1.376
μ(Mo Kα)/cm^{-1}	4.85
no. of collcd data	11 988
no. of indep data	11 598
no.of rflns above 3s(*I*)	4853
no. of refined params	628
goodness of fit	1.52
R	0.059
R_w	0.041

Table 3. Selected Bond Distances (Å) and Angles (deg) for *cis*-3a′

Bond Lengths			
Pd−N3	2.118(5)	Pd−N4	2.106(5)
Pd−C59	2.125(7)	Pd−C61	2.147(7)
Pd−C60	2.085(7)	C59−C60	1.37(1)
C60−C61	1.40(1)		
Bond Angles			
N3−Pd−C59	172.5(3)	N3−Pd−C61	104.8(3)
N4−Pd−C59	103.2(3)	N4−Pd−C61	171.8(3)
N3−Pd−N4	83.4(2)	C59−Pd−C60	68.7(3)
Pd−N3−C14	115.2(5)	Pd−N4−C16	117.5(4)
Pd−N3−C11	131.5(4)	Pd−N4−C19	130.5(4)
C59−C60−C61	121.2(9)		

Dihedral Angles between Least-Squares Planes	
N3PdN4/N1N2N3N4	61.82
N3PdN4/C5C10C15C20	53.40
N1C1C2C3C4/C5C10C15C20	22.08
N2C6C7C8C9/C5C10C15C20	16.94
N3C11C12C13C14/C5C10C15C20	12.63
N4C16C17C18C19/C5C10C15C20	15.88
N1C45C46N2/C5C10C15C20	60.89

plane with the deviation of each atom being less than 0.06 Å from the mean plane. The allyl central carbon C60 deviates by 0.65 Å from the mean plane, while the Pd atom is displaced by 0.03 Å in the opposite direction.

X-ray crystallography shows that the N3−Pd−N4 plane of *cis*-**3a** is canted by 53.4° from the porphyrin plane defined by four meso carbons, C5, C10, C15, and C20. The dihedral angle (106.8°) between the π-allyl plane and the N3−Pd−N4 plane is in the range frequently observed for (π-allyl)palladium complexes.[9−12]

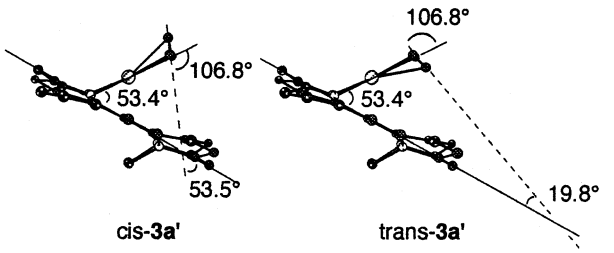

Figure 2. Comparison of the X-ray structure of *cis*-**3a**′ and model of *trans*-**3a**′.

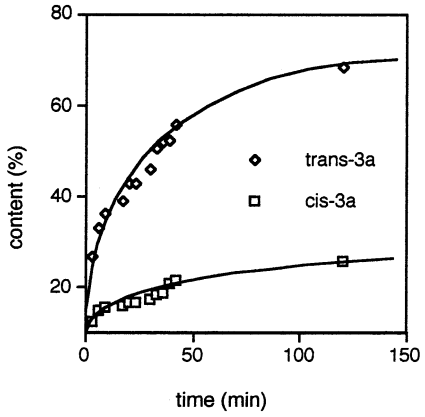

Figure 3. Change in the product distribution (*trans*-**3a** and *cis*-**3a**) with time at −5 °C after addition of (η^1-C_3H_5)-$SnBu_3$ (0.019 M) to **2a** (0.012 M) in $CDCl_3$ (0.5 mL).

If this angle is retained in the trans isomer, the π-allyl plane is presumed to tilt by −19.8° with respect to the porphyrin plane in the trans isomer, while the corresponding tilt angle in the cis isomer is 53.5° (Figure 2).

Kinetics. The progress of the reactions of **2a**,**b** (13 mmol L^{-1}) with allyltributyltin (19 mmol L^{-1}) in $CDCl_3$ was monitored by ^{1}H NMR to show that most of **2a**,**b** has been consumed in 3 min at 25 °C to give the kinetically favored trans isomers as a major component. After this first stage, trans isomers were gradually isomerized to thermodynamically more stable cis isomers until the equilibrium states were reached (vide infra). The amounts of the (π-allyl)Pd^{II} porphyrins were measured with time after allyltributyltin (1.6 equiv) was added to a $CDCl_3$ solution of **2a**,**b** (12 mmol L^{-1}) at −5 °C, at which temperature the trans−cis isomerization could be neglected for the initial 1 h period (Figure 3). Then the second-order rate constants k_1 and k_2 for the formation of *trans*-**3a** and *cis*-**3a** were estimated as 3.2 × 10^{-2} and 1.2 × 10^{-2} L mol^{-1} s^{-1}, and k_1 and k_2 for *trans*-**3b** and *cis*-**3b** were 5.3 × 10^{-2} and 4.0 × 10^{-2} L mol^{-1} s^{-1}, respectively. The difference in the rates of formation between *trans*-**3a** and *cis*-**3a** can be explained in terms of steric hindrance between the tributyltin moiety and the TPP ligand when allyltributyltin approaches Pd. Allyltributyltin in the transition state structure to give (π-allyl)Pd^{II} porphyrins seems to take an orientation where the C−$SnBu_3$ bond undergoes maximum overlap with the C=C π-orbitals. Therefore, the $SnBu_3$ group is far from the porphyrin plane when *trans*-**3a** is being formed, whereas it is closer to the porphyrin plane when *cis*-**3a** is being formed, if the transition state structures are deduced from the X-ray structure of *cis*-**3a**′ as shown in Figure 1. Since the TPP ligand causes greater steric hindrance than the OEP

(8) (a) Smith, A. E. *Acta Crystallogr.* **1965**, *18*, 331. (b) Albinati, A.; Rüegger, H. *Organometallics* **1990**, *9*, 1826. (c) Annibale, G.; Cattalini, L.; Bertolosi, V.; Ferretti, V.; Gestone, G.; Tobe, M. L. *J. Chem. Soc., Dalton Trans.* **1989**, 1265. (d) Murrall, N. W.; Welch, A. J. *J. Organomet. Chem.* **1986**, *301*, 109.

(9) Albinati, A.; Kunz, R. W.; Ammann, C. J.; Pregosin, P. S. *Organometallics* **1991**, *10*, 1800.

(10) Satake, A.; Koshino, H.; Nakata, T. *Organometallics* **1999**, *18*, 5108.

(11) (a) Barbaro, P.; Pregosin, P. S.; Saltmann, R.; Albinati, A.; Kunz, R. W. *Organometallics* **1995**, *14*, 5160. (b) Ramdeehul, S.; Barloy, L.; Osborn, J. A.; De Cian, A.; Fischer, J. *Organometallics* **1996**, *15*, 5442.

(12) (a) Crociani, B.; Bertani, R.; Boschi, T.; Bandoli, G.; *J. Chem. Soc., Dalton Trans.* **1982**, 1715. (b) Togni, A.; Rihs, G.; Pregosin, P. S.; Ammann, C. *Helv. Chim. Acta* **1990**, *73*, 723. (c) Miki, K.; Tanaka, N.; Kasai, N. *J. Organomet. Chem.* **1981**, *208*, 407. (d) Ukhin, L. Y.; Dolgopolova, N. A.; Kuz'mina, L, G.; Struchkov, Y. T. *J. Organomet. Chem.* **1981**, *210*, 263. (e) Facchin, G.; Bertani, R.; Calligaris, M.; Nardin, G.; Mari, M. *J. Chem. Soc., Dalton Trans.* **1987**, 1381.

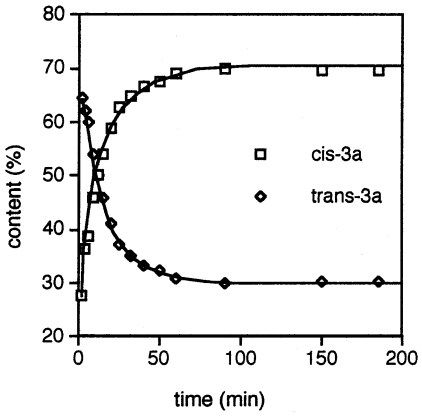

Figure 4. Change in the product distribution (*trans*-**3a** and *cis*-**3a**) with time at 25 °C after addition of (η^1-C_3H_5)-$SnBu_3$ (0.019 M) to **2a** (0.013 M) in $CDCl_3$ (0.5 mL).

ligand, it is reasonable that **2b** reacts faster than **2a** and that the selectivity between *trans*-**3b** and *cis*-**3b** is smaller than that between *trans*-**3a** and *cis*-**3a.**

The reaction of (cyclopent-2-enyl)tributyltin and (2-butenyl)tributyltin was also monitored by observing the decay of **2a**. **4a** and **5a** were formed much more slowly than **3a**, and 2 h was not enough for the complete conversion of **2a**, even at room temperature. The molar ratio at 3 min after the addition of the tin reagent (1.5 equiv) to **2a** in $CDCl_3$ at 25 °C was 0.71:0.15:0.14 for **2a**:*trans*-**4a**:*cis*-**4a**. This trans/cis isomer ratio did not change appreciably when **2a** was allowed to react with the tin reagent (1.8 equiv) for 3 h in CH_2Cl_2 and then chromatographed to afford **4a** in 90% yield. Since the formation of **4a** and **5a** accompanied isomerization at the same time, the formation rates could not be estimated independently.

Isomerization Behavior. As noted above, *trans*-**3a** and *trans*-**3b** formed preferentially were gradually isomerized to *cis*-**3a** and *cis*-**3b**, respectively, until the equilibrium states (both $K_{eq} = 2.3$ for **3a** and **3b**) were reached, as shown in Figure 4. This isomerization process in $CDCl_3$ at 25 °C followed the first-order rate law. The rate constants k_3 for the isomerization from the trans isomer to the cis isomer were determined as 7.1×10^{-4} s^{-1} for **3a** and 4.4×10^{-4} s^{-1} for **3b**.

Ligand rotation in the (π-allyl)palladium(II) complexes has been well-documented. There are two types of π-allyl ligand rotation; one is accompanied by exchange between syn and anti positions, and the other causes exchange between two syn positions and between two anti positions. Syn−anti exchange is frequently observed for the π-allyl ligand of palladium(II) complexes with phosphine ligands.[11,13] It takes place mostly via the $\eta^3-\eta^1$ isomerization mechanism: (i) η^3-to-η^1 allyl coordination change, (ii) rotation around a C−C single bond in the (η^1-allyl)Pd intermediate, and (iii) η^1-to-η^3 allyl coordination change. On the other hand, syn-syn−anti-anti exchange is generally observed for (π-allyl)-palladium(II) complexes with bidentate nitrogen base ligands.[9,14] This exchange is caused by a mechanism

Scheme 2[a]

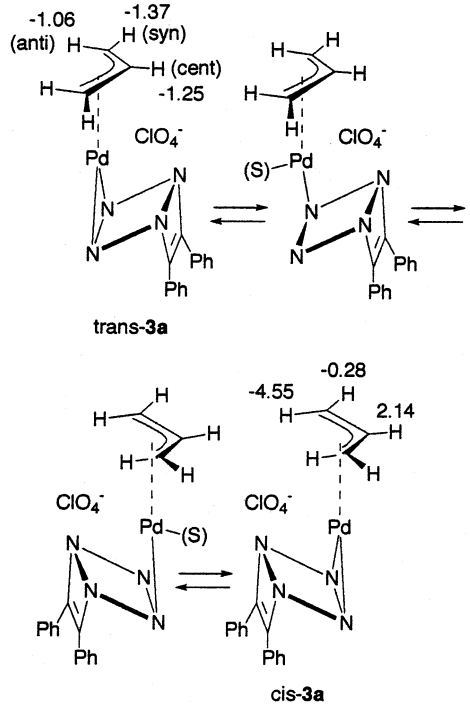

[a] S = solvent.

involving (i) dissociation of one of the Pd−N bonds, followed by (ii) rotation around the remaining Pd−N bond and (iii) remaking of the Pd−N bond as shown in Scheme 2. This difference in the ligand rotation mechanism between amine complexes and phosphine complexes is explained by the fact that the dissociation energy for Pd−N bonds is smaller than that for Pd−P bonds having π-back-bonding.

(a) Syn-Syn−Anti-Anti Exchange. The isomerization mechanism between *trans*-**3a** and cis-**3a** was studied by A phase-sensitive 2D NOESY experiment in tetrachloroethane-d_2 at 80 °C.[9,13,14] The cross-peaks due to chemical exchange between signals at −1.06 ppm ($H_{anti(trans)}$ in Figure 5) and −4.55 ppm ($H_{anti(cis)}$ in Figure 5), between signals at −1.37 ppm ($H_{syn(trans)}$ in Figure 5) and −0.28 ppm ($H_{syn(cis)}$ in Figure 5), and between signals at −1.25 ppm ($H_{cent(trans)}$ in Figure 5) and 2.14 ppm ($H_{cent(cis)}$ in Figure 5) are observed. These negative cross-peaks are indicative of syn-syn−anti-anti exchange. There are no visible cross-peaks between $H_{anti(trans)}$ and $H_{syn(cis)}$ and between $H_{anti(cis)}$ and $H_{syn(trans)}$ that should arise from the syn−anti chemical exchange, whereas correlations between the intramolecular syn and anti π-allyl terminal methylene protons ($H_{syn(cis)}$−$H_{anti(cis)}$ and $H_{syn(trans)}$−$H_{anti(trans)}$) are indicated as positive cross-peaks.

Ligand rotation is detectable if either the (chelating ligand)−Pd or the (π-allyl)−Pd part is nonsymmetric with respect to the plane bisecting the bite angle of the chelating ligand. In the cases of syn-syn−anti-anti exchange, NMR signals due to the halves of the symmetric ligand show different chemical shifts at low temperatures, and they coalesce when the temperature

(13) (a) Breutel, C.; Pregosin, P. S.; Salzmann, R.; Togni, A. *J. Am. Chem. Soc.* **1994**, *116*, 4067. (b) Herrmann, J.; Pregosin, P. S.; Salzmann, R.; Albinati, A. *Organometallics* **1995**, *14*, 3311. (c) Fernández-Galán, R.; Jalón, F. A.; Manzano, B. R.; Rodríguez-de la Fuente, J.; Vrahami, M.; Jedlicka, B.; Weissensteiner, W.; Jogl, G. *Organometallics* **1997**, *16*, 3758.

(14) (a) Gogoll, A.; Örnebro, J.; Grennberg, H.; Bäckvall, J.-E. *J. Am. Chem. Soc.* **1994**, *116*, 3631. (b) Crociani, B.; Antonaroli, S.; Paci, M.; DiBianca, F.; Canovese, L. *Organometallics* **1997**, *16*, 384. (c) Gogoll, A.; Grennberg, H.; Axén, A. *Organometallics* **1997**, *16*, 1167.

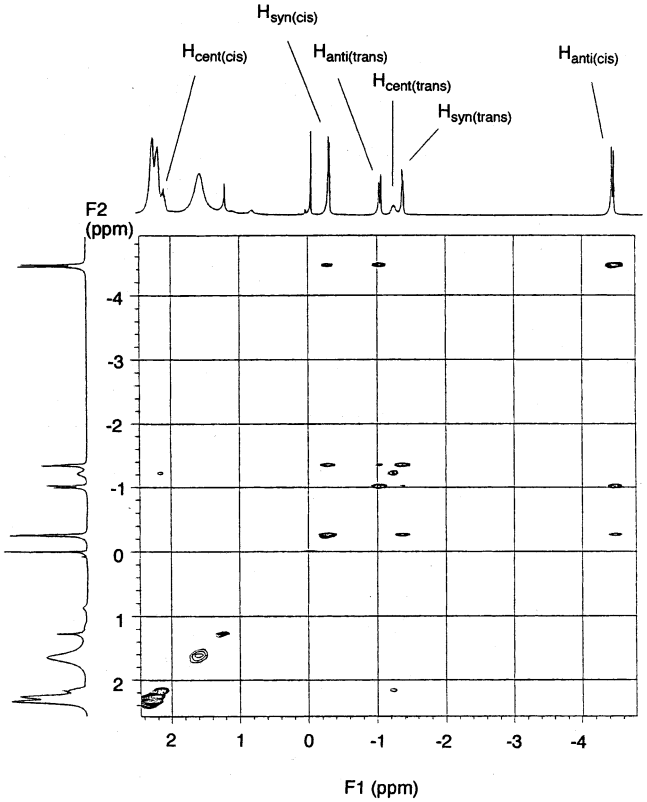

Figure 5. 400-MHz phase-sensitive NOESY spectrum of **3a** in tetrachloroethane-d_2 at 80 °C. The correlations between $H_{anti(cis)}$ and $H_{anti(trans)}$, between $H_{syn(cis)}$ and $H_{syn(trans)}$, and between $H_{cent(cis)}$ and $H_{cent(trans)}$ are observed as negative cross-peaks. Cross-peaks between $H_{anti(cis)}$ and $H_{syn(cis)}$ and between $H_{anti(trans)}$ and $H_{syn(trans)}$ are positive, and all the diagonal peaks are negative.

is raised. Thus, line shape analysis and spin saturation transfer techniques in the dynamic NMR experiments have generally been used for the determination of activation parameters in the ligand rotation.[15] This is partly because ligand rotation is so fast that each isomer cannot be observed separately by NMR at ambient temperature. Furthermore, it is difficult to obtain one rotational isomer as a pure form.

The activation energy for the ligand rotation of **3a** is so large that it can be measured by the concentration change of two rotational isomers with time at ambient temperature. It should be pointed out that two rotational isomers of (π-allyl)Pd complexes are identical if the auxiliary chelating ligand is symmetric with respect to both the plane bisecting the bite angle (L−Pd−L) and the Pd coordination plane, as in the case of 2,2′-bipyridine. This is so even if the π-allyl ligand is unsymmetrically substituted. Although both the (chelating ligand)−Pd and (π-allyl)−Pd parts are symmetric with respect to the plane bisecting the bite angle of the chelating ligand, two rotational isomers of **3a** (cis and trans) can be differentiated due to the unique stereochemical feature of N^{21},N^{22}-bridged porphyrins. It is of great significance that 3/7 *trans*-**3a**/*cis*-**3a** equilibrium mixture in solution is converted into cis-only crystals, owing to the effect of crystal packing. Kinetics of the

Table 4. Equilibrium States between Trans and Cis Conformational Isomers

compd	solvent	temp (°C)	molar ratio (%) trans	molar ratio (%) cis	K_{eq}
3a	$CDCl_3$	25	30	70	2.3
	d_6-DMSO	25	25	75	3.0
	d_6-DMSO	80	34	66	1.9
4a	$CDCl_3$	25	53	47	0.89
	d_6-DMSO	25	29	71	2.4
	d_6-DMSO	80	37	63	1.7
5a					
trans-butenyl	$CDCl_3$	25	7	61	1.8[a]
cis-butenyl			29	3	
trans-butenyl	d_6-DMSO	80	9	87	7.3[a]
cis-butenyl			3	1	

[a] Equilibrium constant between sum of trans isomers (trans(trans) + trans(cis)) and cis isomers (cis(trans) + cis(cis)).

cis-to-trans isomerization could be measured by NMR when the cis isomer was dissolved in $CDCl_3$. An Eyring plot based on the rate constants measured at six different temperatures in the range 278−308 K gave a straight line. On the basis of this plot, $\Delta H^{\ddagger}$ and $\Delta S^{\ddagger}$ values were obtained as 87.7 kJ mol^{-1} and −11.7 J K^{-1} mol^{-1}, respectively, and then the $\Delta G^{\ddagger}$ value of **3a** for this isomerization was calculated as 91.2 kJ mol^{-1} at 298 K.

In the case of syn-syn−anti-anti exchange in the cationic (η^3-*trans*-2-butenyl)Pd^{II} complexes of phenanthroline, the $\Delta G^{\ddagger}_{298}$ value (58.2 kJ mol^{-1}) is obtained on the basis of an Eyring plot ($\Delta H^{\ddagger}$ = 55.0 kJ mol^{-1}; $\Delta S^{\ddagger}$ = −10.6 J K^{-1} mol^{-1}).[15] The syn-syn−anti-anti exchange in the cationic η^3-(2-methylallyl)Pd^{II} complex with the unsymmetrical 2-pyridyl-*N*-benzylimine ligand was investigated by using NMR line shape analysis to give the activation energy E_a = 72 kJ mol^{-1}.[9] It has been pointed out that the activation energy for the syn-syn−anti-anti exchange of the (π-allyl)Pd^{II} complex with neutral pyridinylimidazolyl ligand ($\Delta G^{\ddagger}_{298}$ = 51.8 kJ mol^{-1} in CD_3CN) is smaller than that of the (π-allyl)-Pd^{II} complex with monoanionic pyridinylimidazolate ligand ($\Delta G^{\ddagger}_{298}$ = 69.2 kJ mol^{-1} in CD_3CN).[16] The stronger Pd−N bonding in the latter explains the greater activation energy, because syn-syn−anti-anti exchange requires dissociation of a Pd−N bond. Thus, the remarkably large activation energy $\Delta G^{\ddagger}$ of **3a** may be indicative of the strong Pd−N bonding. Alternatively, it can be explained in terms of steric hindrance of the porphyrin ligand in the rotation around the Pd−N bond followed by the dissociation of one Pd−N bond.

Table 4 shows the effect of solvent and temperature on the equilibrium states between trans and cis isomers of **3a**, **4a**, and **5a**. These complexes were allowed to stand in solution until equilibrium was reached. In the case of **3a** and **4a**, the equilibrium constants (K_{eq}) greatly depend on solvent and of course on temperature. They were 2.3 and 0.89 in $CDCl_3$ and 3.0 and 2.4 in d_6-DMSO at room temperature and 1.9 and 1.7 in d_6-DMSO at 80 °C.

Preference of cis over trans isomers in the case of **3a** may be explained by the greater repulsion between the

(15) Hansson, S.; Norrby, P.-O.; Sjögren, M. P. T.; Åkermark, B.; Cucciolito, M. E.; Giordano, F.; Vitagliano, A. *Organometallics* **1993**, *12*, 4940.

(16) Satake, A.; Koshino, H.; Nakata, T. *Abstracts of the 46th Symposium on Organometallic Chemistry, Japan*; Division of Organometallic Chemistry, Kinki Chemical Society: Osaka, Japan, August 27, 1999; p 112.

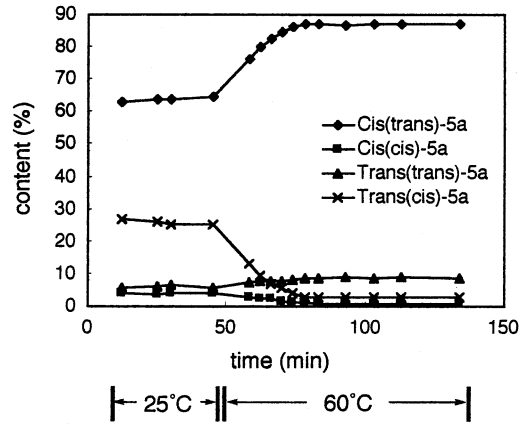

Figure 6. Change in the isomer ratio of butenyl complex **5a** with temperature in d_6-DMSO.

porphyrin ligand and the π-allyl ligand in the trans form than in the cis form. The structures of *cis*-**3a′** and *trans*-**3a′** as depicted in Figure 2 show that the central carbon of the π-allyl group of *trans*-**3a** comes closer to the porphyrin plane than the terminal carbons, because square-planar coordination consists of porphyrin nitrogens and π-allyl terminal carbons. The relative stability of cis and trans isomers is governed mainly by steric repulsion between the π-allyl ligand and the porphyrin ligand.[17] The $-CH_2CH_2-$ part in the η^3-cyclopentenyl ligand of **4a** makes a greater steric constraint in the cis isomer than in the trans isomer, while the central methine of the π-allyl group induces steric repulsion in the trans isomer more than in the cis isomer. The combined steric effect results in the shift of the trans/cis ratio from 30/70 in the complex **3a** to 53/47 in the complex **4a**. The syn methyl substituent in the (η^3-*trans*-2-butenyl)Pd complex **5a** causes steric constraint in the trans isomer but not in the cis isomer, while the anti methyl substituent in the (η^3-*cis*-2-butenyl)Pd complex causes steric constraint in the cis isomer but not in the trans isomer. The observed trans/cis ratio of **5a** in $CDCl_3$ at room temperature is 7/61 in the (η^3-*trans*-2-butenyl)-Pd complex and 29/3 in the (η^3-*cis*-2-butenyl)Pd complex, which is consistent with the above interpretation on the basis of steric repulsion.

(b) Syn−anti Exchange. Figure 6 shows the change in the isomer distribution of **5a** when a d_6-DMSO solution of **5a** was allowed to stand at 25 °C for 45 min and then at 60 °C for 90 min. The trans(cis) isomer decreased as the cis(trans) isomer increased, and the cis(cis) isomer decreased as the trans(trans) isomer increased. This change in the ratio of the four components is explained in terms of the isomerization via a (η^1-allyl)Pd intermediate (see Scheme 3). In this case $\eta^3-\eta^1$ type isomerization is considered to be promoted at 60 °C. This $\eta^3-\eta^1$ type isomerization rate of **5a** could be estimated by using the decrease in sum of the trans(cis) and cis(cis) isomers and the increase in sum of the cis(trans) and trans(trans) isomers. Then the first-order rate constant k_5 for the *cis*-butenyl/*trans*-butenyl isomerization of **5a** via an $\eta^3-\eta^1$ type mechanism at 60 °C was determined as 1.6×10^{-3} s^{-1} ($K_{eq} = 24$). The ratio of cis/trans ligand rotational isomers of the (η^3-*trans*-2-butenyl)Pd complex changes from 65/6 to 87/9 during this temperature change. The corresponding cis/trans ratio of the (η^3-*cis*-2-butenyl)Pd complexes changes from 4/25 to 1/3. These are syn-syn−anti-anti exchange processes. The interconversion between the *trans*-2-butenyl ligand and the *cis*-2-butenyl ligand is a syn−anti exchange process, and the ratio changed from (65 + 6)/(4 + 25) to (87 + 9)/(1 + 3). Therefore, the (η^3-*trans*-2-butenyl)Pd complex is much more stable than the (η^3-*cis*-2-butenyl)Pd complex (Scheme 4). The observed ratio at 25 °C retains the cis/trans composition of the starting (2-butenyl)tributyltin, and an equilibrium state in the (η^3-2-butenyl)Pd porphyrin was not reached due to the very slow syn−anti exchange rate at 25 °C.

The cross-peaks due to syn-syn−anti-anti exchange of **3a** in the phase-sensitive 2D NOESY experiment was observed in tetrachloroethane-d_2 at 80 °C, while it was

Scheme 3[a]

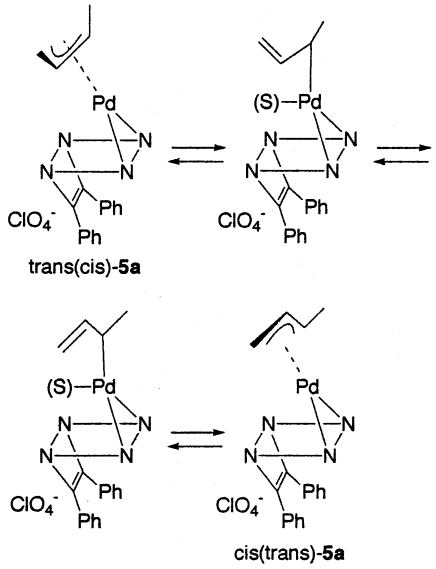

[a] S = solvent.

Scheme 4

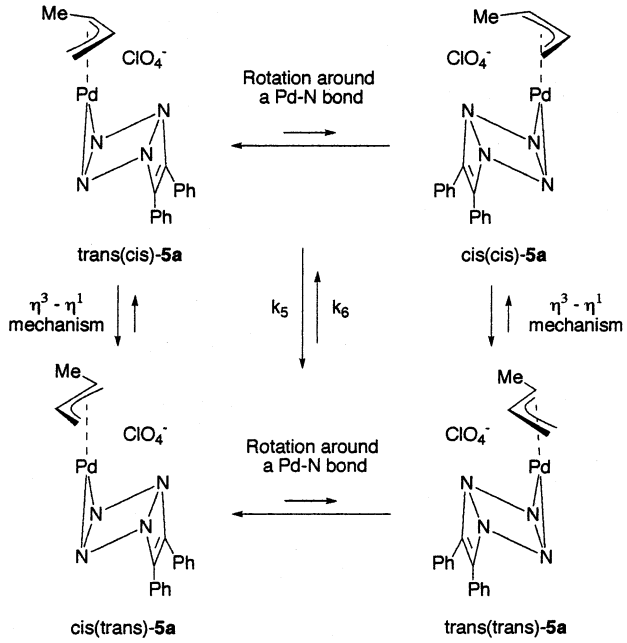

(17) (a) Consiglio, G.; Waymouth, R. M. *Chem. Rev.* **1989**, *89*, 257. (b) Kurosawa, H.; Ogoshi, S.; Kawasaki, Y.; Murai, S.; Miyoshi, M.; Ikeda, I. *J. Am. Chem. Soc.* **1990**, *112*, 2813. (c) Vitagliano, A.; Åkermark, B.; Hansson, S. *Organometallics* **1991**, *10*, 2592.

not detected at room temperature. Since the cross-peaks due to the syn-anti exchange of **3a** could not be detected even in DMSO at 80 °C, the syn-syn−anti-anti exchange is estimated to be much faster than syn-anti exchange under the same conditions. Heating to 140 °C caused decomposition of **3a**. Also in $CDCl_3$ at room temperature, the $\eta^3-\eta^1$ type isomerization of **5a** is slower than syn-syn−anti-anti isomerization. This fact agrees with the result reported for the (π-2-butenyl)Pd^{II} complex with the 1,10-phenanthroline ligand in tetrachloroethane-d_2, in which the rate constant for $\eta^3-\eta^1$ type isomerization ($k_{298} = 2.8 \times 10^{-3}$ s^{-1}) is much smaller than that for syn-syn−anti-anti isomerization ($k_{298} = 396$ s^{-1}).[15] A much slower syn-syn−anti-anti isomerization of porphyrin Pd complexes as compared to that of 1,10-phenanthroline complexes can be ascribed to the steric hindrance of the porphyrin ligand in the rotation around the Pd−N bond, because it does not seem that the Pd to porphyrin nitrogen bonding is stronger than the Pd to 1,10-phenanthroline nitrogen bonding. $\eta^3-\eta^1$ type isomerization does not involve dissociation of a Pd−N bond and would not be greatly affected by the steric hindrance of the porphyrin ligand. Therefore, the rate constant for this type of isomerization is diagnostic of the trans effect of porphyrin nitrogens. That is, strong Pd−N bonding should lead to fast $\eta^3-\eta^1$ type isomerization. Since the $\eta^3-\eta^1$ type isomerization of **5a** is not faster than that for the phenanthroline complex, the Pd−N bonding of **5a** does not seem to be much stronger than that of phenanthroline. This is consistent with the structural feature of **3a** that the Pd−N bondings are bent by 21.8 and 23.7° from the pyrrole ring planes.

Conclusion

Bis(perchlorato)Pd^{II} complexes of N^{21},N^{22}-etheno-bridged porphyrins reacted with allyltins, resulting in the formation of (π-allyl)palladium(II) derivatives with N^{21},N^{22}-bridged porphyrin ligands. The substituent at the allyl moiety exerted influence on the equilibrium state of two product isomers with different orientations of π-allyl ligands relative to the porphyrin ligand. The rate for syn-syn−anti-anti isomerization of the π-allyl ligand of Pd(II) porphyrin is remarkably slower than those for (π-allyl)Pd^{II} complexes with ordinary nitrogen base ligands. The porphyrin ring current effect greatly helps differentiating two isomers and thus elucidating isomerization behaviors. The present study shows the great possibilities of N^{21},N^{22}-bridged porphyrin as a ligand stereochemically controlling the reactivity of organo ligands by covering one side of the square plane of Pd coordination.

Experimental Section

General Considerations. (Dichloro)palladium(II) complexes of N^{21},N^{22}-etheno-bridged porphyrins **1a**−**c** were synthesized according to the previously reported procedures.[5] Solvents were purified prior to use by conventional methods. $CDCl_3$ was passed through basic Al_2O_3 before use. (Cyclopent-2-enyl)tributyltin was a gift from Dr. H. Miyake (Kobe University). (2-Butenyl)tributyltin was synthesized by the Grignard reaction of tributyltin chloride with 1-chloro-2-butene. Other chemicals were of reagent grade. Wakogel C-300 silica gel (Wako Junyaku) was used for column chromatography. ^1H NMR spectra were recorded on JEOL EX-270 and AL-300 spectrometer. Chemical shifts were referenced with respect to $(CH_3)_4Si$ (0 ppm) as an internal standard. The UV−visible spectra were measured on a Shimadzu UV-3100B instrument. Elemental analyses of C, H, and N were made with a Yanaco MT-5 and Perkin-Elmer 2400 CHN corder. FAB mass spectra were measured in an *m*-nitrobenzyl alcohol matrix with a JEOL-JNS 600 instrument, and ESI-MS spectra were measured with a Mariner PE Biosystems spectrometer. X-ray crystallographic measurement was done on Rigaku AFC-5 automated four-circle diffractometer.

Caution! The compounds prepared here are perchlorates that involve the risk of an explosion and must be handled with extreme caution.

General Procedure for Preparation of Bis(perchlorato)palladium(II) Porphyrins (2a−c). A mixture of **1a**−**c** (0.05 mmol), $AgClO_4$ (0.05 mmol), and dichloromethane (5 mL) was stirred vigorously at room temperature. The white precipitate of AgCl appeared within 1 h. AgCl was filtered off after stirring for 3 h. The filtrate was evaporated, and the product was recrystallized from dichloromethane−hexane.

(N^{21},N^{22}-PhC=CPh-TPP)Pd(ClO_4)$_2$ (2a). ^1H NMR (300 MHz, $CDCl_3$): δ 9.35, 8.91, 8.68, 8.20 (d × 4, 2H × 4, β-Py H), 8.66−7.31 (m, 20H, Ph meso-H), 6.22 (t, 2H, bridge Ph p-H), 5.77 (br, 4H, bridge Ph m-H). Anal. Calcd for $C_{58}H_{38}N_4O_8Cl_2Pd\cdot 2H_2O$: C, 58.72; H, 4.08; N, 4.72. Found: C, 58.49; H, 4.00; N, 4.53. UV−vis (CH_2Cl_2; nm): 652.5, 633.0, 589.0, 463.5, 413.0. ESI MS (*m*/*z*): found 995.30, theory 995.15 for $C_{58}H_{38}N_4O_4ClPd$ ($(M - ClO_4)^+$).

(N^{21},N^{22}-PhC=CPh-OEP)Pd(ClO_4)$_2$ (2b). ^1H NMR (300 MHz, $CDCl_3$): δ 11.14, 10.59, (s × 2, 1H × 2, meso-H), 10.12 (s, 2H, meso-H), 4.47−3.63 (m, 16H, CH_2), 2.31, 1.85, 1.39, 1.25 (t × 4, 6H × 4, CH_3), 6.03 (t, 2H, bridge Ph p-H), 5.56 (br, 4H, bridge Ph m-H). Anal. Calcd for $C_{50}H_{54}N_4O_8Cl_2Pd\cdot 2H_2O$: C, 55.18; H, 5.74; N, 5.15. Found: C, 55.59; H, 5.62; N, 4.59.

(N^{21},N^{22}-EtC=CEt-TPP)Pd(ClO_4)$_2$ (2c). ^1H NMR (300 MHz, $CDCl_3$): δ 9.17, 8.78, 8.76, 8.55 (d × 4, 2H × 4, β-Py H), 8.53−7.85 (m, 20H, Ph meso-H), −1.36 (t, 6H, bridge CH_3), −2.85, −4.27 (dq × 2, 2H × 2, bridge CH_2, $J_{gem} = 15$ Hz). Anal. Calcd for $C_{50}H_{38}N_4O_8Cl_2Pd\cdot 4H_2O$: C, 54.19; H, 4.55; N, 5.06. Found: C, 54.28; H, 4.40; N, 5.05. FAB MS (*m*/*z*): found 899, theory 899 for $C_{50}H_{38}N_4O_4PdCl$ ($(M - ClO_4)^+$).

General Procedure of Synthesis of (π-Allyl)palladium(II) Porphyrins (3a−5a). Allyltributyltin derivatives (0.025 mmol) were added to a solution of **2a** (0.014 mmol) in dichloromethane (2 mL). After the mixtures were stirred for 3 h, the products were purified by column chromatography on silica gel with dichloromethane−acetone (7/1) as an eluent. Recrystallization from dichloromethane−hexane gave the mixtures of trans and cis isomers of (π-allyl)palladium(II) porphyrins.

The TPP free base form, N^{21},N^{22}-PhC=CPh-TPP, was prepared by vigorously mixing a CH_2Cl_2 solution of a monoprotonated form, (N^{21},N^{22}-PhC=CPh-TPP)$HClO_4$, with a 10% KOH solution.[5] Then the free base was allowed to react with $[Pd(C_3H_5)Cl]_2$ (1.1 equiv) in benzene at room temperature overnight to give [(1,2-diphenyletheno-N^{21},N^{22})-*meso*-tetraphenylporphyrinato-N^{23},N^{24}](η^3-allyl)palladium(II) chloride (**3a′**) in a 90% isolated yield, after evaporation of benzene and precipitation using CH_2Cl_2 and hexane.

($N,^{21}N^{22}$-PhC=CPh-TPP)(η^3-allyl)Pd(ClO_4) (3a). ^1H NMR (300 MHz, $CDCl_3$): δ 9.14, 8.87, 8.73, 8.22 (d × 4, 2H × 4, β-Py H of *trans*-**3a**), 9.11, 8.80, 8.75, 8.18 (d × 4, 2H × 4, β-Py H of *cis*-**3a**), 8.44−7.31 (m, Ph meso-H of *trans*-**3a** and *cis*-**3a**), 6.26 (t, bridge Ph p-H of *trans*-**3a** and *cis*-**3a**), 5.82 (br, bridge Ph m-H of *trans*-**3a** and *cis*-**3a**); see Table 1 for the allyl protons. Anal. Calcd for $C_{61}H_{43}N_4O_4ClPd$: C, 70.59; H, 4.18; N, 5.40. Found: C, 70.39; H, 3.98; N, 5.35. UV−vis (CH_2Cl_2; λ_{max}, nm (log ϵ)): 668.5 (4.15), 625.0 4.23), 572.0 (4.09), 468.0 (5.15), 409.5 (4.95). FAB MS (*m*/*z*): found 937, theory 937 for $C_{61}H_{43}N_4Pd$ ($(M - ClO_4)^+$) (an observed isotopic pattern agrees with that simulated for $C_{61}H_{43}N_4Pd$).

(N^{21},N^{22}-PhC=CPh-TPP)(η^3-cyclopentenyl)Pd(ClO_4) (4a). ^{1}H NMR (300 MHz, $CDCl_3$): δ 9.16, 9.10, 8.83, 8.82, 8.72, 8.71, 8.20, 8.10 (d × 8, 2H × 8, β-Py H of *trans*-**4a** and *cis*-**4a**), 8.39−7.28 (m, Ph meso-H of *trans*-**4a** and *cis*-**4a**), 6.20 (t × 2, bridge-Ph p-H of *trans*-**4a** and *cis*-**4a**), 5.79 (br, bridge Ph m-H of *trans*-**4a** and *cis*-**4a**); see Table 1 for the cyclopentenyl protons. Anal. Calcd for $C_{63}H_{45}N_4O_4ClPd\cdot 2H_2O$: C, 68.79; H, 4.49; N, 5.09. Found: C, 68.70; H, 4.19; N, 5.04. UV−vis (CH_2Cl_2; λ_{max}, nm (log ε)): 671.0 (4.45), 624.5 (4.51), 565.0 (4.43), 466.0 (5.42), 414.0 (5.32). FAB MS (*m*/*z*): found 963, theory 963 for $C_{63}H_{45}N_4Pd$ ($(M - ClO_4)^+$) (an observed isotopic pattern agrees with that simulated for $C_{63}H_{45}N_4Pd$).

(N^{21},N^{22}-PhC=CPh-TPP)(η^3-butenyl)Pd(ClO_4) (5a). ^{1}H NMR (300 MHz, $CDCl_3$): δ 9.12−7.20 (β-Py H and Ph meso-H of four isomers were not assigned by overlap of signals), 6.20 (t × 2, bridge Ph p-H of *trans*-**5a** and *cis*-**5a**), 5.80 (br, bridge Ph m-H of *trans*-**5a** and *cis*-**5a**); see Table 1 for the butenyl protons. Anal. Calcd for $C_{62}H_{47}N_4O_4ClPd\cdot H_2O$: C, 69.47; H, 4.61; N, 5.23. Found: C, 69.24; H, 4.60; N, 5.19. UV−vis (CH_2Cl_2; λ_{max}, nm (log ε)): 673.0 (4.23), 629.0 (4.28), 573.5 (4.11), 469.5 (5.15), 414.0 (5.05). ESI MS (*m*/*z*): found 951.2757, theory 951.2694 for $C_{62}H_{45}N_4Pd$ ($(M - ClO_4)^+$).

General Procedure of Preparation for (Perchlorato)-palladium(II) Porphyrins (6a−c). A mixture of **1a** (0.05 mmol), $AgClO_4$ (0.2 mmol), and dichloromethane (5 mL) was stirred vigorously at room temperature. The white precipitate of AgCl appeared within 1 h. The workup procedure was the same as for **2a**−**c**.

[(N^{21},N^{22}-PhC=CPh-TPP)PdCl]$_2$(ClO_4)$_2$ (6a). ^{1}H NMR (300 MHz, $CDCl_3$): δ 9.41, 8.49, 8.47, 7.69 (d × 4, 2H × 4, β-Py H), 8.39−7.03 (m, 20H, Ph meso-H), 5.98 (t, 2H, bridge Ph p-H), 5.49 (br, 4H, bridge Ph m-H). Anal. Calcd for $C_{58}H_{38}N_4O_4Cl_2Pd\cdot H_2O$: C, 66.33; H, 3.84; N, 5.33. Found: C, 66.29; H, 3.80; N, 5.31. UV−vis (CH_2Cl_2; λ_{max}, nm): 655.0, 603.5, 461.5, 407.5. ESI-MS (*m*/*z*): found 963.1429; theory 963.2093 for $C_{59}H_{42}N_4OClPd$ ($((M - 2ClO_4)/2 + CH_3OH)^+$).

[(N^{21},N^{22}-PhC=CPh-OEP)PdCl]$_2$(ClO_4)$_2$ (6b). ^{1}H NMR (300 MHz, $CDCl_3$): δ 10.77, 10.20, (s × 2, 1H × 2, meso-H), 9.15 (s, 2H, meso-H), 4.28−3.34 (m, 16H, CH_2), 1.38, 1.15, 0.97, 0.94 (t × 4, 6H × 4, CH_3), 5.73 (t, 2H, bridge Ph p-H), 5.17 (br, 4H, bridge Ph m-H). Anal. Calcd for $C_{50}H_{54}N_4O_4Cl_2Pd$: C, 63.06; H, 5.72; N, 5.88. Found: C, 62.94; H, 5.83; N, 5.48. ESI-MS (*m*/*z*): found 852.2066, theory 852.3082 for $C_{50}H_{54}N_4ClPd$ ($((M - 2ClO_4)/2)^+$).

[*N*,^{21}N^{22}-(EtC=CEt)(TPP)PdCl]$_2$(ClO_4)$_2$ (6c). ^{1}H NMR (300 MHz, $CDCl_3$): δ 9.06, 8.33, 8.18, 8.06 (d × 4, 2H × 4, β-Py-H), 8.10−7.08 (m, 20H, meso-Ph-H), −1.87 (t, 6H, bridge-CH_3), −3.52, −5.12 (dq × 2, 2H × 2, bridge-CH_2, J_{gem} = 15 Hz). Anal. Calcd for $C_{50}H_{38}N_4O_4Cl_2Pd\cdot 2H_2O$: C, 61.77; H, 4.35; N, 5.76. Found: C, 61.93; H, 4.71; N, 5.24. FAB MS (*m*/*z*): found 1772 and 836, theory 1772.9 for $C_{100}H_{76}N_8O_4Cl_3Pd_2$ ($(M - ClO_4)^+$) and 836.3 for $C_{50}H_{38}N_4ClPd$ ($((M - 2ClO_4)/2)^+$).

Physicochemical Measurements. The rate constants for the formation of (π-allyl)Pd porphyrins **3a**,**b** and their trans−cis isomerization were determined by NMR experiments. (allyl)$SnBu_3$ (9×10^{-6} mol) was added to a 0.5 mL $CDCl_3$ solution of **2a**,**b** (5−6 μmol) in a NMR tube, just after which the sample tube was transferred to a thermostated NMR spectrometer at 25 or 5 °C. The changes in concentrations of the components in the solution were estimated on the basis of ^{1}H NMR integrations with time. For the determination of the thermodynamic parameters for cis-to-trans isomerization of **3a**, 5 μmol of *cis*-**3a** was dissolved in 0.5 mL of $CDCl_3$ in a NMR tube, and the change in the isomer ratio was monitored with time at six different temperatures (5, 10, 15, 25, 28, and 35 °C). The observed rate constants were used for the Eyring plot that is included in the Supporting Information. The η^3−η^1 type isomerization of **5a** was detected using a d_6-DMSO solution (0.5 mL) of 3.8 μmol of the mixture of four isomers. The sample tube was kept at 25 °C for 45 min and then heated to 60 °C. NMR measurements were repeated four times at 25 °C and 11 times at 60 °C to make sure that isomer distribution reaches a constant value.

The 400 MHz phase-sensitive 2D NOESY spectrum of **3a** was measured using a mixing time of 0.3 s in tetrachloroethane-d_2 at 80 °C.

A crystal of **3a′** obtained by recrystallization from CH_2Cl_2−hexane was mounted on an X-ray diffractometer, and measurements were done using graphite-monochromated Mo Kα radiation. The unit cell parameters were obtained from least-squares refinements of 8 reflections ($20.3 < 2\theta < 26.2°$). The intensities of 3 representative reflections which were measured after every 150 reflections showed a 0.85% increase over the course of data collection. The data were corrected for Lorentz and polarization effects and absorption based on azimuthal scans. The refined cell parameters and relevant crystal data are summarized in Table 2. The structure was solved by direct methods and refined by full-matrix least-squares methods (Texsan[18]) on an SGI R-5000 workstation. All non-hydrogen atoms were refined anisotropically. Hydrogen atoms were included at standard positions (C−H = 0.95 Å) but not refined. Neutral atom scattering factors were taken from Cromer and Waber.[19] Anormalous dispersion effects were included in F_c; the values for $\Delta f'$ and $\Delta f''$ were those of Cromer.[20] The atomic coordinates with *B*(eq), *U* values, bond distances, bond angles, torsional angles, and least-squares planes are given in Tables 2−7 in the Supporting Information.

Acknowledgment. This work was supported by a grant-in-aid for scientific research (No. 12440186) from the Ministry of Education, Science, Sports, and Culture of Japan. We thank Prof. H. Miyake (Kobe University) for the gift of (cyclopentenyl)tributyltin and Ms. M. Nishinari (Kobe University) for analytical work. We are also grateful to Dr. M. Sawada, Mr. H. Yamada, and Mrs. F. Fukuda (MAC, ISIR, Osaka University) for FAB MS analysis and elemental analysis.

Supporting Information Available: Tables of crystallographic data, atomic coordinates, anisotropic thermal parameters, and torsion angles of *cis*-**3a′** and figures giving theESI-MS spectrum of **6b** and an Eyring plot based on the kinetic measurements relating to the isomerization of **3a**. This material is available free of charge via the Internet at http://pubs.acs.org.

OM0205593

(18) Texsan-Texray Structure Analysis Package; Molecular Structure Corp., The Woodlands, TX, 1985.
(19) Cromer, D. T.; Waber, J. T. *International Tables for X-ray Crystallography*; Kynoch Press: Birmingham, England, 1974; Vol. IV, Table 2.2A.
(20) Cromer, D. T.; Waber, J. T. *International Tables for X-ray Crystallography*; Kynoch Press: Birmingham, England, 1974; Vol. IV, Table 2.3.1.